K_a-Band Rotational Spectroscopy of Succinimide and N-Chlorosuccinimide

Chisom A. Dim,[†] Caroline Sorrells,[‡] Alicia O. Hernandez-Castillo,[‡] and Kyle N. Crabtree[*,†]

†*Department of Chemistry, University of California, Davis, Davis, California, 95616, United States*

‡*Department of Chemistry, Harvey-Mudd College, Claremont, California, 91711, United States*

E-mail: kncrabtree@ucdavis.edu

Abstract

Succinimide and its derivatives are cyclic five-membered rings that appear in a variety of natural products and are widely used in organic synthesis. From a structural standpoint, succinimide contains an NH group in the ring which interacts with two adjacent carbonyl groups, pushing the ring structure toward planarity at the expense of increasing ring strain and eclipsing interactions among the out-of-plane hydrogen atoms in the two CH_2 groups. Previous quantum chemical calculations at different levels of theory have predicted both a nonplanar C_2 structure and a planar C_{2v} structure, the latter of which is the most consistent with gas-phase electron diffraction measurements. Here, we report the pure rotational spectra of succinimide and N-chlorosuccinimide in the 26.5–40.0 GHz range using chirped-pulse Fourier transform microwave spectroscopy, supported by coupled cluster and density functional theory quantum chemical calculations. The spectra were fit to Watson's A-reduced effective Hamiltonian, including both

^{35}Cl and ^{37}Cl isotopologues of N-chlorosuccinimide as well as the N and Cl quadrupole hyperfine interactions. On the basis of the agreement with quantum chemical calculations and the measured inertial defects, we find that the rotational spectra are consistent with a planar ring structure, with a maximum out-of-plane angle of $\leq 5^{\circ}$.

Introduction

Understanding the preferred molecular geometry and the dynamic equilibrium between the structures in the conformational landscape of a molecule is useful for exploring a wide range of properties relevant to biological activity[1] and organic synthesis.[2] Succinimide is a 5-membered saturated heterocyclic compound in which an endocyclic secondary amine group (−NH) is between two carbonyl groups (−C=O, Figure 1). Succinimide derivatives are found in many natural products[3] and in pharmaceuticals as antibacterial, anti-inflammatory, antimicrobial, antitumor, and antiviral agents.[4] Succinimide-based anticonvulsants like ethosuximide, phensuximide, and methsuximide have also been used against absence seizures.[5,6] In addition, polyalkenylamide-succinimides are useful as anticorrosion coatings for processing metallic materials in the construction industry.[7] Moreover, N-halosuccinimides are very popular in organic chemistry for their use as halogenating agents for aromatic compounds[8] and as reagents for functional group transformations.[9,10]

Five-membered rings have rich conformational dynamics and serve as prototypical model systems for understanding the conformational landscape of more complex molecules.[11] A selection of cyclopentane derivatives containing an endocyclic heteroatom and/or carbonyl groups is shown in Figure 1. The bare five-membered rings (row a. Figure 1), cyclopentane, tetrahydrofuran, and pyrrolidine, all feature pseudorotation, a large amplitude motion involving the atoms of the ring. Cyclopentane can assume either a twisted/half-chair nonplanar conformer with C_2 symmetry or an envelope/bent-ring structure with C_s symmetry slightly higher in energy ($\Delta E = 175$ cm^{-1}), and undergoes free pseudorotation between the two conformers.[11–14] The presence of substituents on the cyclopentane ring and the incorpo-

ration of heteroatoms within the ring alter the conformational preference and pseudorotation dynamics.[15] Upon insertion of an oxygen atom into the ring, for example, a slight barrier to pseudorotation of 50 cm^{-1} arises,[16–20] while inclusion of a nitrogen atom results in a much greater pseudorotation barrier of 581 cm^{-1}.[21–24]

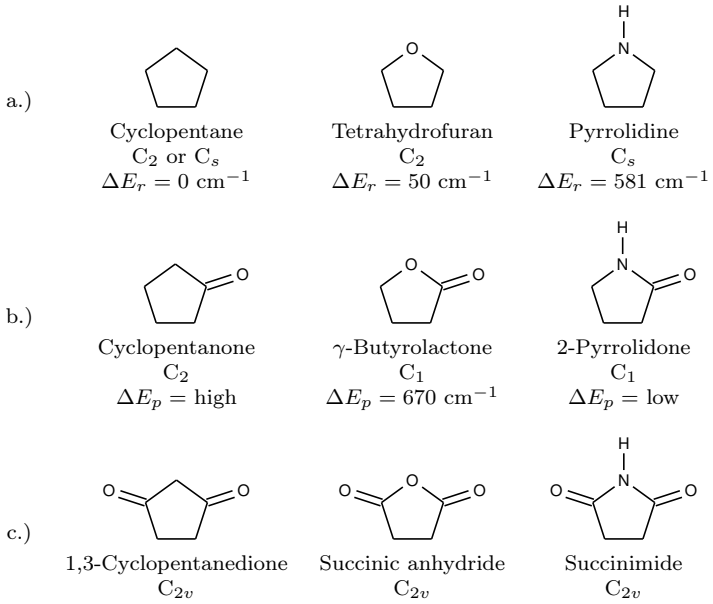

Figure 1: Symmetries, pseudorotation barriers (ΔE_r), and/or puckering barriers (ΔE_p) of saturated cyclopentane derivatives.

The next family of molecules (row b. Figure 1) contains one –C=O group: cyclopentanone, γ-butyrolactone, and 2-pyrrolidone. The presence of an sp^2-hybridized C atom in the ring prevents the pseudorotation motion, but these rings may feature ring puckering involving a carbon atom two positions away from the –C=O group. For cyclopentanone,[25–28] no splitting from large amplitude motion was observed in its microwave spectrum evidencing a high barrier to ring puckering (estimated value: 750 cm^{-1} [29]). The ring puckering barrier is lower for γ-butyrolactone (670 cm^{-1})[30,31] and lower still in 2-pyrrolidone (2–21 cm^{-1} from semiempirical calculations).[32,33] The impact of a second –C=O group (row c. in Figure 1), such as in succinimide is less well explored. There are no high-resolution studies of 1,3-cyclopentanedione, but a solid-state X-ray diffraction study[34] found a planar-heavy-atom structure. Succinic anhydride has been recently measured by rotational spectroscopy and

is currently thought to have a C_{2v} equilibrium geometry, though it has been the subject of some controversy.[35,36]

Despite its ubiquity in medicine and in organic synthesis, succinimide has not been investigated by high resolution spectroscopy. Gas-phase electron diffraction (GED) measurements for succinimide are consistent with a heavy atom planar structure.[37] However, the GED results do not inform about the presence or absence of interesting ring conformational dynamics. Moreover, in contrast to succinic anhydride, the heteroatom in succinimide can be functionalized, providing a handle to explore how the electronic properties of the substituent may impact the ring structure. We have previously studied the rotational spectrum of N-ethyl-succinimide,[38] which was found to be consistent with a heavy-atom planar structure. Here, we report the pure rotational spectra of succinimide and N-chlorosuccinimide measured by chirped-pulse Fourier transform microwave spectroscopy. Interpretation of the spectra is aided by both ab initio and density functional theory quantum chemical calculations.

Experimental Methods

Samples of succinimide (99.1%) and N-chlorosuccinimide (98%) were purchased from Sigma Aldrich and used without further purification. The rotational spectra of the succinimides were acquired using a K_a-band (26.5 - 40 GHz) chirped-Pulse Fourier transform microwave spectrometer which has been described previously.[39] Both samples are solids at room temperature, and to raise their vapor pressure, approximately 0.5 grams were loaded into a heated reservoir located about 5 cm behind a pulsed solenoid valve. The vapor from the sample was entrained in a flow of argon at a pressure of 3.8 bar and pulsed at a repetition rate of 5 Hz into a vacuum chamber with a base pressure of $\sim 10^{-6}$ Torr. Each gas pulse was irradiated with twenty 2 μs chirps at high power ($\sim$150 W) spaced by 20 μs, and the resultant free induction decays (FIDs) were digitized at 50 GSa/s and co-averaged. The total record length of each FID was 12 μs. First, the spectrum was continuously monitored as the temperature

of the reservoir was increased until a maximum signal strength was obtained. After the optimal temperature was determined, a second experiment was performed at that temperature, which was ∼140 ± 10℃ for both species. The total acquisition time/total FIDs collected was 2 hrs/766,260 and 1.5 hrs/527,100 for succinimide and N-chlorosuccinimide respectively. The Fourier transform of the co-averaged FIDs was scaled by a polynomial representing the instrument response function and was analyzed using Pickett's SPFIT/SPCAT programs[40] to determine the experimental spectroscopic parameters.

Computational Methods

To guide the interpretation of the experimental rotational spectrum, geometry optimizations for succinimide were performed at the coupled-cluster (CCSD(T)) level of theory with the cc-pwCVTZ[41,42] basis set. Due to the computational expense of evaluating CCSD(T)/cc-pwCVTZ vibration-rotation corrections, we intended to perform such calculations with the cc-pVDZ basis set. However, the geometry optimization with this smaller basis set converged to a C_2 equilibrium geometry, while the cc-pwCVTZ structure was C_{2v}. We therefore carried out density functional theory (DFT) geometry optimizations with a variety of functionals and basis sets, all of which yielded C_{2v} structures. Vibration-rotation corrections were then computed at the B3LYP[43]/6-311+G(2d,p)[44] level of theory. Based on the agreement with experimental spectroscopic constants (vide infra), we focus primarily on the CCSD(T)/cc-pwCVTZ and ωB97x-D/def2-TZVP[45,46] optimized geometries with B3LYP/6-311+G(2d,p) vibration-rotation corrections for succinimide. Results from other levels of theory are provided in the Supporting Information. A similar strategy was adopted for N-chlorosuccinimide.

The MP2 and coupled cluster calculations were carried out with a development version of the CFOUR program.[47] Geometry optimizations were performed with a convergence threshold of 10^{-10} Hartrees/Bohr and harmonic frequency calculations were carried out for all the

optimized geometries except the triple-zeta CCSD(T) calculations. DFT calculations were performed using the Gaussian 16 program with an ultrafine grid and the "VeryTight" convergence setting[48]. For succinimide, equilibrium rotational constants and dipole moment projections were computed at the CCSD(T)/cc-pwCVTZ and ωB97x-D/def2-TZVP optimized geometries; for N-chlorosuccinimide, the CCSD(T) calculations employed the Jorge TZP basis set.[49] Vibration-rotation corrections and quartic centrifugal distortion terms for both molecules were evaluated from force constants computed at the B3LYP/6-311+G(2d,p) level of theory.

Results

Succinimide

The equilibrium geometries from the MP2 and CCSD(T) calculations using the double zeta cc-pVDZ basis set both converged to a C_2 puckered structure, and the absence of imaginary harmonic frequencies confirmed that each C_2 structure is a local minimum. Focusing on the CCSD(T) results, the puckering dihedral angle $\angle$(H11-N0-C1-C2) (according to the atom numbering scheme shown in Figure 2) was found to deviate from planarity by only 2.4°. By performing a geometry optimization with the symmetry constrained to C_{2v}, a transition state with an imaginary puckering frequency of $32.9i$ cm^{-1} and an energy only 2 cm^{-1} above that of the calculated C_2 equilibrium geometry was obtained. Such a low transition state energy, coupled with a ring puckering frequency of only 46 cm^{-1} for the C_2 structure, suggest that the potential (shown in the Supporting Information) is quite flat near the planar structure at this level of theory, which is consistent with earlier MP2/6-311G(d,p) calculations[37]. The MP2/cc-pVDZ and CCSD(T)/cc-pVDZ structures and frequencies are provided in the Supporting Information.

The calculated structural parameters of succinimide at the CCSD(T)/cc-pwCVTZ and ωB97x-D/def2-TZVP levels are shown in Table 1. Unlike the double zeta calculations,

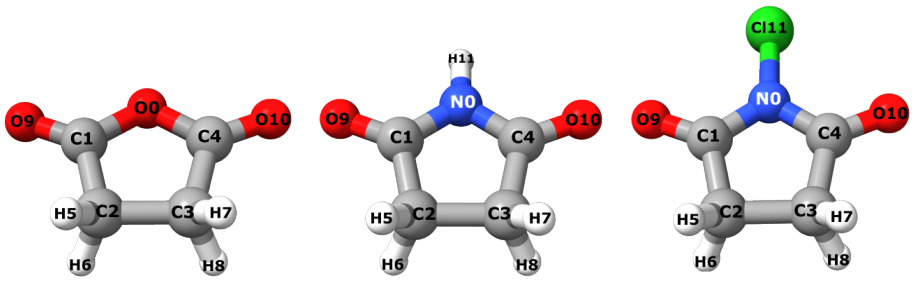

Figure 2: ωB97x-D/def2-TZVP structures of succinic anhydride, succinimide, and N-chlorosuccinimide (left to right).

both converged to a ring-planar C_{2v} geometry; nevertheless, the ring-puckering vibrational mode at the ωB97x-D/def2-TZVP level has a quite low frequency of 85 cm^{-1} suggesting the potential is indeed quite flat. Table 1 also shows the structural parameters of succinimide as determined by experimental GED measurements.[37] The CCSD(T) and ωB97x-D calculations are in excellent agreement with the experimental structure: bond lengths agree to within $\sim$0.01 Å and angles to within 1.5°.

The calculated equilibrium rotational constants and dipole moment projections for succinimide are shown in Table 2, along with the ground-state vibrational corrections to the rotational constants. Succinimide is a somewhat prolate asymmetric top with an asymmetry parameter value of $\kappa = -0.72$ and a moderate dipole moment of nearly 2 D oriented along the b inertial axis, resulting in a purely b-type rotational spectrum. It is worth noting that the C_2 structures predicted by the double zeta calculations also possess a dipole moment purely along the b axis. The question of whether the equilibrium structure of succinimide is ring-planar or puckered cannot be directly addressed by a search for c-type transitions. The vibrational corrections are all negative with a value of just under 1% of their corresponding rotational constants, which is within the typical range for small semi-rigid molecules.

The 26.5–40 GHz rotational spectrum of succinimide is shown in Figure 3. The quality of the calculated ground-state constants made the spectral assignment process straightforward. The most striking feature in the experimental spectrum is the quartet of lines near 38 GHz.

Table 1: Structural parameters of succinimide. Bond lengths in Å, angles in degrees. Parameters are labeled with respect to the structure in Figure 2.

Parameter	GED[37]	CC[a]	DFT[b]
R(C4-O10)	1.202(1)	1.205	1.199
R(C1-N0)	1.376(2)	1.388	1.384
R(C1-C2)	1.520(4)	1.521	1.519
R(C2-C3)	1.526(5)	1.532	1.529
R(C2-H5)	1.086(7)	1.088	1.089
R(N0-H11)	1.007(18)	1.007	1.008
∠(C1-N0-C4)	116.5(4)	115.0	115.0
∠(C1-N0-H11)	121.8(2)	122.5	122.5
∠(N0-C1-O9)	126.1(4)	125.2	125.1
∠(N0-C1-C2)	106.3(3)	107.1	107.1
∠(O9-C1-C2)	127.6(2)	127.7	127.8
∠(C1-C2-C3)	105.5(2)	105.4	105.4
∠(C1-C2-H5)	109.7(14)	108.4	108.4
∠(C2-C3-H7)	112.7(12)	113.4	113.6
∠(H5-C2-H6)	106.5(29)	107.5	107.3
∠(H5-C2-C1-N0)	±121.7(14)	±121.8	±121.9
∠(H11-N0-C4-O10)	0.00	0.00	0.00
Symmetry	C_{2v}	C_{2v}	C_{2v}

[a] CCSD(T)/cc-pwCVTZ
[b] ωB97x-D/def2-TZVP

Table 2: Calculated equilibrium rotational constants, dipole projections, and vibration-rotation corrections for succinimide and N-chlorosuccinimide.

	Succinimide		^{35}Cl-succinimide		^{37}Cl-succinimide	
Parameter	CC[a]	DFT[b]	CC[c]	DFT[b]	CC[c]	DFT[b]
A_e (MHz)	5959.1	5969.9	2245.0	2262.4	2245.0	2262.4
B_e (MHz)	2267.2	2283.7	1968.5	1985.4	1914.1	1930.6
C_e (MHz)	1676.2	1686.0	1062.6	1071.4	1046.5	1055.2
$\mu_a/\mu_b/\mu_c(D)$	0/1.9/0	0/2.1/0	3.1/0/0	3.3/0/0	3.1/0/0	3.3/0/0
ΔA^d (MHz)	45.1		13.9		13.9	
ΔB^d (MHz)	13.1		11.4		11.4	
ΔC^d (MHz)	9.4		5.9		5.9	
A_0 (MHz)	5913.9	5924.7	2231.1	2248.5	2231.1	2248.5
B_0 (MHz)	2254.1	2270.6	1957.1	1974.0	1902.7	1919.2
C_0 (MHz)	1666.8	1676.6	1056.7	1065.4	1040.6	1049.3

[a] CCSD(T)/cc-pwCVTZ
[b] ωB97x-D/def2-TZVP
[c] CCSD(T)/TZP
[d] B3LYP/6-311+G(2d,p)

At a first glance, it would appear that these lines are all related to one another, but it turns out this is not the case. The doublet in the center corresponds to the $11_{0,11}$ - $10_{1,10}$ and $11_{1,11}$ - $10_{0,10}$ transitions and it is flanked by the $9_{2,8}$ - $8_{1,7}$ and $5_{3,3}$ - $4_{2,2}$ transitions which happen to be almost equally spaced relative to the doublet. Nevertheless, these were readily predicted in the theoretical spectrum and initially assigning these four transitions immediately brought the rest of the simulated spectrum into qualitative agreement with the experiment. The primary progression appearing in this frequency range, shown in red in Figure 3, consists of the $J'_{0,J'}$ - $J''_{1,J''}$ and $J'_{1,J'}$ - $J''_{0,J''}$ R-branch doublets from $J'' = 7$ to 10, whose spacing decreases with increasing J. Many lines in the spectrum showed resolvable hyperfine splitting due to the presence of the quadrupolar nitrogen nucleus which was readily analyzed.

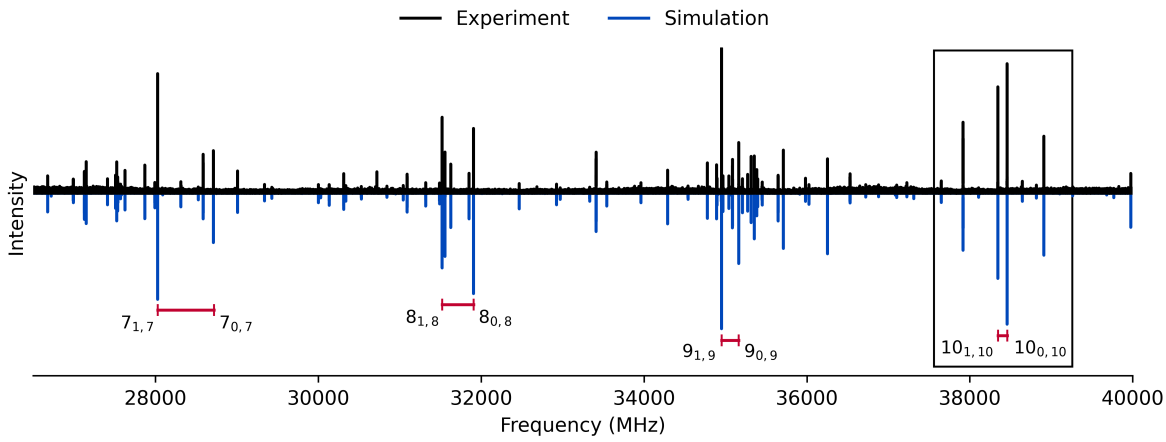

Figure 3: K_a band rotational spectrum of succinimide (black) and simulated spectrum at T = 7K (blue). Spectral features discussed in the main text are indicated by the red lines and the box. Labels on transitions refer to the $J''_{K''_a,K''_c}$ values.

In addition, the effect of nuclear spin statistical weights (NSSWs) on the line intensities from the presence of indistinguishable hydrogen nuclei was observed in the spectrum. For succinimide, a C_{2v} geometry gives rise to four equivalent protons, while a C_2 geometry would instead give two separate pairs of equivalent protons. Nevertheless, in both cases the combinations of symmetry-allowed nuclear spin functions with rotational functions gave the same statistical weights: 10 for states with K_a and K_c both even or both odd, and 6 for

states with one even and the other odd. The NSSWs give rise to a 5:3 intensity ratio in the spectrum which is observed experimentally, yet they do not directly discriminate between the ring-planar and nonplanar structures. The simulation shown in Figure 3 contains these NSSWs, and a rotational temperature of 7 K was found to give an overall excellent intensity agreement with the experimental spectrum.

A total of 164 transitions were fit to Watson's A-reduced effective Hamiltonian[50] in the I^r representation with a root mean square (RMS) error of 25.8 kHz (Table 3). Given the experimental full-width half-max linewidth of ∼180 kHz, the line center frequencies were assigned a uniform uncertainty of 20 kHz. In addition to the rotational constants, the complete set of quartic centrifugal distortion constants and the diagonal elements of the nitrogen hyperfine tensor were well-determined. A comparison with the calculated parameters shows excellent agreement with both levels of theory employed here: rotational constants agree to within 0.4%, the distortion constants agree to within 6.0%, and the hyperfine constants agree to within 2.0%. These values represent the maximum deviations between both levels of theory. A second fit using the S-reduction (see Supporting Information) yielded similar results, giving confidence that the analysis is robust.

N-chlorosuccinimide

As with succinimide, the MP2 and CCSD(T) calculations for N-chlorosuccinimide with the cc-pVDZ basis set resulted in C_2 equilibrium structures; the C_{2v} structures at these levels of theory were only about 10 cm^{-1} higher in energy and had an imaginary vibrational frequency corresponding to the puckering coordinate. The geometry computed with the larger TZP basis set converged to the C_{2v} structure. Table 4 shows the structural parameters of N-chlorosuccinimide calculated with CCSD(T)/TZP and ωB97x-D/def2-TZVP methods. Similar to succinimide, the computed structures are in semi-quantitative agreement with the GED measurements.

The rotational spectrum for N-chlorosuccinimide is shown in Figure 4. Both isotopologues

Table 3: Experimental and theoretical spectroscopic constants (A reduction, I^r representation) for the ground vibrational state of succinimide. Numbers in parenthesis are 1σ uncertainties in units of the last digit.

Parameter	Experiment	CC[a]	DFT[b]
A_0 (MHz)	5922.8921(11)	5913.93	5924.74
B_0 (MHz)	2264.15367(66)	2254.15	2270.57
C_0 (MHz)	1673.14190(61)	1666.78	1676.56
Δ_J (kHz)	0.0938(31)	0.09[c]	
Δ_{JK} (kHz)	0.2950(63)	0.28[c]	
Δ_K (kHz)	1.663(40)	1.66[c]	
δ_J (kHz)	0.02531(60)	0.02[c]	
δ_K (kHz)	0.226(11)	0.23[c]	
χ_{aa} (MHz)	1.229(26)	1.24	1.20
χ_{bb} (MHz)	1.7491(74)	1.80	1.79
χ_{cc} (MHz)	−2.9781(74)	−3.04	−2.99
Δ_0(uÅ^2)[d]	−6.48	−6.45	−6.44
RMS (kHz)[e]	25.80		
N_f^f	164		
J''_{max}/J''_{min}	17/2		
$K''_{a,max}/K''_{a,min}$	4/0		

[a] CCSD(T)/cc-pwCVTZ
[b] ωB97x-D/def2-TZVP
[c] B3LYP/6-311+G(2d,p)
[d] Inertial defect, $\Delta = I_c - I_b - I_a$.
[e] Root mean square deviation of observed and calculated frequencies.
[f] Number of unique frequencies in the fit.

Table 4: Structural parameters of N-chlorosuccinimide. Bond lengths in Å, angles in degrees. Parameters are labeled with respect to the structure in Figure 2.

Parameter	GED[51]	CC[a]	DFT[b]
R(C1-O9)	1.201(2)	1.200	1.193
R(C1-N0)	1.401(2)	1.401	1.398
R(C1-C2)	1.515(2)	1.519	1.515
R(C2-C3)	1.530(2)	1.534	1.529
R(C2-H5)	1.106(18)	1.089	1.089
R(N0-Cl11)	1.672(3)	1.686	1.672
∠(C1-N0-C4)	114.7(5)	115.6	115.4
∠(N0-C1-C2)	106.8(3)	106.2	106.3
∠(C1-C2-C3)	105.9(2)	106.0	106.0
∠(N0-C1-O9)	123.7(5)	125.3	125.3
∠(C1-C2-C3-C4)	0.00	0.00	0.00
Symmetry	C_{2v}	C_{2v}	C_{2v}

[a]CCSD(T)/TZP
[b]ωB97x-D/def2-TZVP

of chlorine, ^{35}Cl and ^{37}Cl are observed in their natural abundance of 75% to 25%. The spectrum also features succinimide, which presumably arises as a result of the decomposition of N-chlorosuccinimide upon heating. Halosuccinimides are frequently employed in organic synthesis for accessing functionality at the nitrogen position because the halogen is a good leaving group. Upon heating in the present experiment, presumably, the halogen is replaced by a hydrogen atom coming from residual moisture, despite efforts to ensure dry conditions. Efforts to observe N-bromosuccinimide and N-iodosuccinimide both resulted in spectra of succinimide as bromine and iodine are even better leaving groups.

N-chlorosuccinimide is heavier and more oblate than succinimide, and its rotational spectrum is accordingly richer in the 26.5-40 GHz region. It is dominated by a series of seven R-branch, a-type, near-oblate band heads separated by approximately 2.1 GHz, with J'' values from 11 to 17 and K_a'' values from 0 to 8 (the strongest transitions have $K_c'' = 2$). Each band begins with a degenerate pair of $J'_{0,J'} - J''_{0,J''}$ and $J'_{1,J'} - J''_{1,J''}$ transitions, and as the band progresses toward lower frequency, the J values decrease, the K_a values increase, and transitions with the same K_c value show asymmetry splitting.

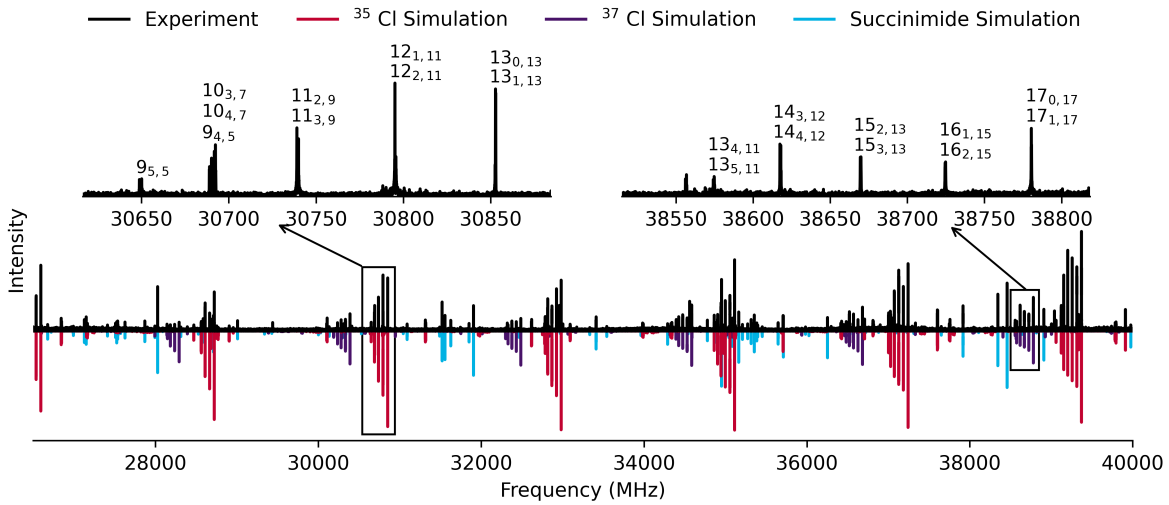

Figure 4: K_a-band rotational spectrum of N-chlorosuccinimide (black). Spectral simulations show contributions from the ^{35}Cl (red) and ^{37}Cl (purple) isotopologues, as well as from succinimide (blue). Simulations are at a rotational temperature of 7 K. Insets show details of R branch head structures for ^{35}Cl (left) and ^{37}Cl (right) isotopologues. Labels refer to $J''_{K''_a,K''_c}$ values.

Given the obvious band structures, assignment of rotational quantum numbers to the ^{35}Cl isotopologue transitions was straightforward. The presence of a second quadrupolar chlorine nucleus in addition to the nitrogen gives rise to additional splitting in the rotational spectrum as illustrated in Figure 5. The largest splitting arises from the chlorine nucleus with the nitrogen adding small splittings to the overall Cl structure. The substantial difference in splittings between the two nuclei greatly facilitated the assignment and fitting of the complex hyperfine structure in the spectrum. Similar to succinimide, the NSSWs for the C_{2v} and C_2 geometries both yield identical statistical weights; however, the symmetry axis in N-chlorosuccinimide is instead the a inertial axis. The NSSWs are therefore 10:6 for states with K_a = even:odd, respectively. Overall, the intensities observed in the experimental spectrum were best reproduced with a rotational temperature of 7 K. A total of 353 transitions were fit to Watson's A-reduced effective Hamiltonian in the III^l representation, achieving an RMS error of 25.9 kHz (Table 5). A second fit in the S-reduction achieved nearly identical results and is included in the Supporting Information.

Following the ^{35}Cl isotopologue analysis, predictions for the rotational constants of the

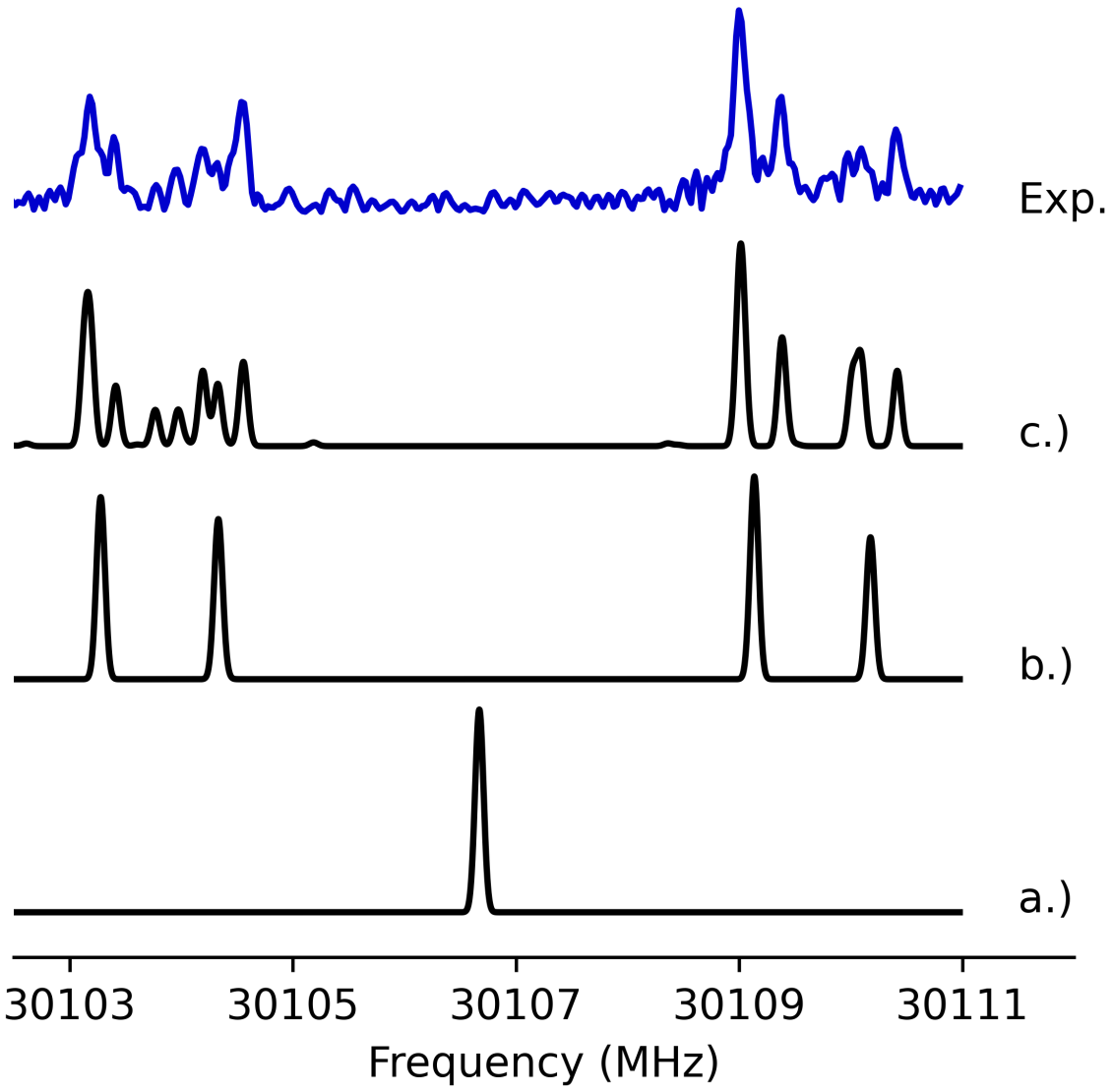

Figure 5: Simulated (black) and experimental (blue, top) rotational spectrum of the 9_{64} - 8_{63} transition of N-chlorosuccinimide. a.) pure rotational transition, b.) inclusion of the ^{35}Cl hyperfine splitting, and c.) inclusion of both ^{35}Cl and ^{14}N hyperfine splitting.

Table 5: Experimental and theoretical spectroscopic constants (A reduction, III^l representation) for the ground vibrational state of two isotopologues of N-chlorosuccinimide. Numbers in parenthesis are 1σ uncertainties in units of the last digit and those in brackets were fixed in the fit.

Parameter	^{35}Cl			^{37}Cl		
	Experiment	CC[a]	DFT[b]	Experiment	CC[a]	DFT[b]
A_0 (MHz)	2243.13999(51)	2231.12	2248.53	2243.1528(30)	2231.12	2248.53
B_0 (MHz)	1975.94949(46)	1957.12	1974.03	1921.5734(28)	1902.69	1919.24
C_0 (MHz)	1064.88734(59)	1056.65	1065.43	1048.88833(79)	1040.59	1049.27
Δ_J (kHz)	0.1349(27)	0.15[c]		0.1329(61)	0.15[c]	
Δ_{JK} (kHz)	0.1805(92)	0.16[c]		[0.1805]	0.16[c]	
Δ_K (kHz)	−0.2962(67)	-0.29[c]		−0.2950(67)	-0.29[c]	
δ_J (kHz)	[0.0026]	0.0026[c]		[0.0026]	0.0026[c]	
δ_K (kHz)	−1.4775(99)	-1.34[c]		−1.227(47)	-1.34[c]	
χ_{aa}^{Cl} (MHz)	−109.727(21)	−113.15	−115.20	[−86.3992]	−89.18	−90.79
χ_{bb}^{Cl} (MHz)	55.657(21)	57.25	58.52	[43.8244]	45.12	46.12
χ_{cc}^{Cl} (MHz)	54.07(09)	55.90	56.68	[42.5748]	44.06	44.67
χ_{aa}^{N} (MHz)	4.5194(43)	4.51	4.69	[4.5194]	4.51	4.69
χ_{bb}^{N} (MHz)	0.1626(43)	0.02	0.02	[0.1626]	0.02	0.02
χ_{cc}^{N} (MHz)	−4.682(32)	−4.53	−4.70	[−4.682]	−4.53	−4.70
Δ_0(uÅ^2)[d]	−6.48	−6.45	−6.43	−6.48	−6.46	−6.43
RMS (kHz)[e]	25.95			30.89		
N_f^f	353			92		
J''_{max}/J''_{min}	17/6			17/8		
$K''_{a,max}/K''_{a,min}$	9/0			6/0		

[a] CCSD(T)/TZP

[b] ωB97xD/def2-TZVP

[c] B3LYP/6-311+G(2d,p)

[d] Inertial defect, $\Delta = I_c - I_b - I_a$.

[e] Root mean square deviation of observed and calculated frequencies.

[f] Number of unique frequencies in the fit.

^{37}Cl isotopologue were obtained by scaling the best fit experimental rotational constants of the ^{35}Cl isotopologue by the ratio of ^{37}Cl and ^{35}Cl rotational constants from the quantum chemical calculations. Because the chlorine nucleus lies directly along the a inertial axis, both the A rotational constant and the ratios of the inertial components of the quadrupolar nuclei remain unchanged; the χ tensor elements of the chlorine nucleus were scaled by the ratio of the quadrupole moments of ^{35}Cl and ^{37}Cl.[52,53]

After making these two scalings, the simulated spectrum was already in near-perfect agreement with the experiment. A total of 92 transitions were then identified and assigned, fewer than the parent isotopologue owing to the lower natural abundance of ^{37}Cl. Because of the smaller number of transitions, it was not possible to simultaneously fit all of the spectroscopic parameters. For the fit shown in Table 5, all of the hyperfine parameters and the Δ_{JK} and δ_J centrifugal distortion terms were held equal to the values determined for the ^{35}Cl isotopologue. Despite the lower signal-to-noise ratio, the RMS error of the fit was 30.89 kHz.

Discussion

Given the conformational flexibility and puckering dynamics observed in other five-membered rings (Figure 1), it is of interest to consider to what extent succinimide and/or other cyclic 1,3-diones display similar behavior. From a structural standpoint, the presence of sp^2-hybridized carbon atoms at non-adjacent positions within the succinimide ring favors a planar arrangement, but this comes at the energetic cost of unfavorable eclipsing interactions of the CH_2 groups and the cost of forcing the nitrogen in the secondary amine to adopt an sp^2 hybridization. Our CCSD(T)/cc-pVDZ calculations gave rise to C_2 structures with puckering dihedral angles of only a few degrees for succinimide and N-chlorosuccinimide, but at higher levels of theory a ring-planar C_{2v} structure was favored. In the rotational spectrum, the signal strength was insufficient to afford detection of the ^{13}C isotopologues in

natural abundance, so a semi-experimental structure determination is not directly possible from the current results.

The inertial defect $\Delta = I_c - I_b - I_a$ provides a measure of non-planarity, as its value is zero for a perfectly planar structure. For example, maleimide, which differs from succinimide by the presence of a double bond between C2 and C3 (Figure 1), is planar with C_{2v} symmetry. Its experimentally measured ground-state inertial defect is only -0.05 amu Å^2,[54] with the small negative value arising due to zero-point vibrational motion involving out-of-plane bending modes. The experimental inertial defects for both succinimide and N-chlorosuccinimide align with the expected inertial defect associated with the four out-of-plane hydrogens of the two CH_2 groups (-6.48 amu Å^2, Tables 3 and 5).[55] For reference, the experimental inertial defect for succinic anhydride was found to be -6.62 amu Å^2.[35,36] Figure S2 shows the calculated inertial defect at the ωB97x-D/def2-TZVP level of theory as a function of the puckering dihedral angle, based on a series of constrained optimizations. These values include the B3LYP/6-311+G(2d,p) vibration-rotation corrections evaluated at the C_{2v} geometry, under the assumption that the α values would not change significantly for small puckering angles. The experimental inertial defects are consistent with a puckering angle of $\lesssim 5°$. The main source of uncertainty comes from the exact CH bond lengths and angles.

The structure of succinic anhydride, which has an oxygen atom in place of the NH group in succinimide, has been a subject of debate. McMahon et al.[35] recorded the pure rotational spectrum of succinic anhydride and observed nearly uniform splittings of order 100 kHz for all transitions in the spectrum. They attributed this splitting to a pseudorotation of the puckered ring structure; their calculated B2PLYPD3/6-311++G(d,p) equilibrium geometry had a puckering angle of about 0.5°. However, Jahn et al.[36] have called this interpretation into question. Similar to the quantum chemical calculations reported here for succinimide, the calculated equilibrium structure of succinic anhydride is heavy-atom planar at some levels of theory and non-planar at others. Jahn et al. found that at the CCSD(T)/cc-pwCVTZ equilbrium structure of succinic anhydride is puckered by about 1.1°, but the

puckering angle decreases to 0.3° with the larger cc-pwCVQZ basis set. DFT calculations give a heavy-atom planar C_{2v} structure. A reinvestigation of the pure rotational spectrum at higher spectral resolution with a Balle-Flygare microwave spectrometer revealed that low-J rotational transitions were split into multiplets with spacings of order 10 kHz, while higher-J transitions showed no splitting. Jahn et al. attributed these splittings to spin-spin coupling among the out-of-plane hydrogen atoms which collapses with increasing J. Although precise spin-spin coupling parameters were not determined from the spectrum, they would be a sensitive probe of the heavy-atom structure of the succinic anhydride ring.

Given the structural similarity between succinimide and succinic anhydride, succinimide is calculated to have nearly identical spin-spin coupling parameters involving the out-of-plane hydrogen atoms (Table 6). Those for N-chlorosuccinimide are likewise very similar in magnitude, but are rotated due to the change in inertial axis orientation. In our K_a band rotational spectra, all observed splittings can be attributed purely to hyperfine splitting from the quadrupolar nuclei: N for succinimide, and also Cl for N-chlorosuccinimide. However, given the experimental linewidths which arise from our perpendicular jet configuration and the larger J values of the transitions in our frequency range, splittings from spin-spin coupling would be too small to resolve. Measurement of low-J transitions of succinimide and N-chlorosuccinimide at high spectral resolution may afford additional insight into the heavy-atom-planar structure of the succinimide ring. The quadrupole hyperfine parameters derived in this work would be helpful in deconvolving the expected complex line splitting patterns.

Given the delicate balance of ring strain, eclipsing interactions, and stabilization of the sp^2 hybridization of the nitrogen atom in succinimide, modifications to the electronic structure may alter the preferred ring structure. We have previously investigated the structure of N-ethylsuccinimide by rotational spectroscopy and quantum chemical calculations; the results were, like succinimide, consistent with a heavy-atom-planar structure.[38] The chlorine atom in N-chlorosuccinimide is electron-withdrawing, which may diminish the stabilization afforded by conjugation of the nitrogen p orbital with the carbonyl groups. Indeed, the

Table 6: Calculated nuclear spin-nuclear spin coupling terms for the optimized C_{2v} structures of succinic anhydride (MP2/aug-cc-pVTZ), succinimide (CCSD(T)/cc-pwCVTZ), and N-chlorosuccinimide (CCSD(T)/TZP), in kHz. Hydrogen pairs are numbered according to Figure 2.

H pairs	Term	Succinic anhydride[36]	Succinimide	N-chlorosuccinimide
7–8/9–10	$\frac{3}{2}D_{aa}$	33.45	33.31	33.10
	$\frac{1}{4}(D_{bb}-D_{cc})$	16.73	16.65	16.55
7–10/8–9	$\frac{3}{2}D_{aa}$	−6.58	−6.54	6.88
	$\frac{1}{4}(D_{bb}-D_{cc})$	1.21	1.20	−1.03
7–9/8–10	$\frac{3}{2}D_{aa}$	−26.46	−26.14	13.16
	$\frac{1}{4}(D_{bb}-D_{cc})$	0.00	0.00	−6.58

orbital shape for the nitrogen non-bonding orbital in N-chlorosuccinimide shows a decrease in conjugation relative to that for succinimide (Figure S1). In addition, the harmonic frequency of the lowest-frequency A_2 mode, corresponding to the out-of-plane puckering of the CH_2 groups, is lower in N-chlorosuccinimide than in succinimide, with a larger positive anharmonic correction (Tables S6 and S7). These differences in the vibrational potential suggest that replacement of Cl with an even stronger electron-withdrawing group may cause a C_2-like ring structure to become favored over the C_{2v} framework.

Conclusions

We have investigated the structure of the five-membered heterocyclic ring molecules succinimide and N-chlorosuccinimide via a combination of rotational spectroscopy in the 26.5 - 40 GHz frequency range and quantum chemical calculations. The overall agreement of the derived rotational parameters with theoretical CCSD(T) and ωB97x-D structures is excellent, and the results are overall consistent with a heavy-atom planar ring structure with a puckering angle of less than 5°. Splittings observed in the experimental spectra were accounted for by nitrogen and/or chlorine hyperfine splittings, and neither species displays evidence of splitting arising from large-amplitude motion at the present spectral resolution. Improved experimental constraints on the planarity of the ring may be afforded by resolving spin-

spin coupling among the out-of-plane hydrogen atoms in low-J transitions (as observed in succinic anhydride[36]) and/or determining a semiexperimental equilibrium structure with isotopic substitution. Finally, the presence of more strongly electron-withdrawing substituents on the nitrogen may favor a puckered geometry of the five-membered succinimide ring.

Keywords

Rotational spectroscopy, molecular structure, ring puckering

Supporting Information

S-reduction fits, calculated rotational parameters, vibrational frequencies, orbital isosurface diagrams, and inertial defect plots (PDF).

Computational outputs, spectroscopic fitting program outputs, rotational spectra (ZIP).

Acknowledgements

This work was supported by a grant from the National Science Foundation number AST-2042257. This work used Bridges-2 at the Pittsburgh Supercomputing Center through allocation CHE220068 from the Advanced Cyberinfrastructure Coordination Ecosystem: Services & Support (ACCESS) program, which is supported by National Science Foundation grants #2138259, #2138286,#2138307, #2137603, and #2138296.

References

(1) Jampilek, J. Heterocycles in medicinal chemistry. 2019.

(2) Cabrele, C.; Reiser, O. The modern face of synthetic heterocyclic chemistry. *J. Org. Chem.* **2016**, *81*, 10109–10125.

(3) Sakkani, N.; Nanda, S. K. A review on the synthesis and applications of α-alkylidene succinimides. *Asian J. Org. Chem.* **2022**, *11*, e202200041.

(4) Sharma, U.; Kumar, P.; Kumar, N.; Singh, B. Recent advances in the chemistry of phthalimide analogues and their therapeutic potential. *Mini Rev Med Chem* **2010**, *10*, 678–704.

(5) Macdonald, R.; McLean, M. Anticonvulsant drugs: mechanisms of action. *Adv. neurol. neurosci.* **1986**, *44*, 713–736.

(6) Löscher, W.; Schmidt, D. Modern antiepileptic drug development has failed to deliver: ways out of the current dilemma. *Epilepsia* **2011**, *52*, 657–678.

(7) Boev, E. V.; Islamutdinova, A. A.; Aminova, E. K. Development of Technology for Obtaining Anticorrosive Nanostructured Polyalkenylamide-Succinimide Coatings in Construction. *Nanotekhnologii v Stroitel'stve* **2023**, *15*, 6–13.

(8) Larock, R. C. *Comprehensive Organic Transformations*; Wiley, 1989.

(9) Booker-Milburn, K. I.; Fedouloff, M.; Paknoham, S. J.; Strachan, J. B.; Melville, J. L.; Voyle, M. A new Claisen sequence for the synthesis of 3-substituted-2-oxindoles. *Tetrahedron Lett.* **2000**, *41*, 4657–4661.

(10) Ranu, B. C.; Jana, U. A new redundant rearrangement of aromatic ring fused cyclic α-hydroxydithiane derivatives. Synthesis of aromatic ring fused cyclic 1, 2-diketones with one-carbon ring expansion. *J. Org. Chem.* **1999**, *64*, 6380–6386.

(11) Durig, J.; Zhao, W. In *Structures and Conformations of Non-Rigid Molecules*; Laane, J., Dakkouri, M., van der Veken, B., Oberhammer, H., Eds.; Springer, 1993; pp 113–136.

(12) Adams, W. J.; Geise, H. J.; Bartell, L. S. Structure, equilibrium conformation, and pseudorotation in cyclopentane. An electron diffraction study. *J. Am. Chem. Soc.* **1970**, *92*, 5013–5019.

(13) Dragojlovic, V. Conformational analysis of cycloalkanes. *ChemTexts* **2015**, *1*, 14.

(14) Pitzer, K. S.; Donath, W. E. Conformations and strain energy of cyclopentane and its derivatives. *J. Am. Chem. Soc.* **1959**, *81*, 3213–3218.

(15) Altona, C. *Conformational analysis. Scope and present limitations*; Academic Press New York London, 1971.

(16) Mamleev, A.; Gunderova, L.; Galeev, R. Microwave spectrum and hindered pseudorotation of tetrahydrofuran. *J. Struct. Chem.* **2001**, *42*, 365–370.

(17) Engerholm, G. G.; Luntz, A. C.; Gwinn, W.; Harris, D. O. Ring Puckering in Five-Membered Rings. II. The Microwave Spectrum, Dipole Moment, and Barrier to Pseudorotation in Tetrahydrofuran. *J. Chem. Phys.* **1969**, *50*, 2446–2457.

(18) Meyer, R.; López, J. C.; Alonso, J. L.; Melandri, S.; Favero, P. G.; Caminati, W. Pseudorotation pathway and equilibrium structure from the rotational spectrum of jet-cooled tetrahydrofuran. *J. Chem. Phys.* **1999**, *111*, 7871–7880.

(19) Geise, H. J.; Adams, W. J.; Bartell, L. S. Electron diffraction study of gaseous tetrahydrofuran. *Tetrahedron* **1969**, *25*, 3045–3052.

(20) Almenningen, A.; Seip, H.; Willadsen, T.; Heinegård, D.; Balaban, A. T.; Craig, J. C. Studies on Molecules with Five-membered Rings. II. An Electron Diffraction Investigation of Gaseous Tetrahydrofuran. *Acta Chem. Scand.* **1969**, *23*, 2748–2754.

(21) Caminati, W.; Oberhammer, H.; Pfafferott, G.; Filgueira, R. R.; Gomez, C. H. The microwave spectrum of pyrrolidine. *J. Mol. Spectrosc.* **1984**, *106*, 217–226.

(22) Caminati, W.; Dell'Erba, A.; Maccaferri, G.; Favero, P. G. Free jet absorption millimeter wave spectrum of pyrrolidine: assignment of a second, equatorial, the most stable conformer. *J. Mol. Spectrosc.* **1998**, *191*, 45–48.

(23) Pfafferott, G.; Oberhammer, H.; Boggs, J. E.; Caminati, W. Geometric structure and pseudorotational potential of pyrrolidine. An ab initio and electron diffraction study. *J. Am. Chem. Soc.* **1985**, *107*, 2305–2309.

(24) Kunitski, M.; Riehn, C.; Matylitsky, V. V.; Tarakeshwar, P.; Brutschy, B. Pseudorotation in pyrrolidine: rotational coherence spectroscopy and ab initio calculations of a large amplitude intramolecular motion. *Phys. Chem. Chem. Phys.* **2010**, *12*, 72–81.

(25) Tamagawa, K.; Hilderbrandt, R.; Shen, Q. Molecular structure of cyclopentanone by gas-phase electron diffraction. *J. Am. Chem. Soc.* **1987**, *109*, 1380–1383.

(26) Kim, H.; Gwinn, W. D. Ring Puckering in Five-Membered Rings. III. The Microwave Spectrum, Dipole Moment, and Structure of Cyclopentanone. *J. Chem. Phys.* **1969**, *51*, 1815–1819.

(27) Mamleev, A. K.; Gunderova, L.; Pozdeev, N. Microwave spectrum of cyclopentanone-113C,-213C, and-313C and the structure of the ring. *J. Struct. Chem.* **1979**, *19*, 642–644.

(28) Erlandsson, G. Microwave Spectrum of Cyclopentanone. *J. Chem. Phys.* **1954**, *22*, 563–564.

(29) Ikeda, T.; Lord, R. C. Far-Infrared Spectra of Ring Compounds. IX. Far-Infrared Spectrum and Hindered Pseudorotation in Cyclopentanone. *J. Chem. Phys.* **1972**, *56*, 4450–4466.

(30) Durig, J.; Li, Y.; Tong, C. C. Spectra and structure of small ring compounds: XXIX. Microwave spectrum of γ-butyrolactone. *J. Mol. Struct.* **1973**, *18*, 269–275.

(31) Alonso, J. L.; Cervellati, R.; Degli Esposti, A.; Palmieri, P. Conformation and ring inversion in -butyrolactone. *J. Chem. Soc. Faraday Trans.* **1990**, *86*, 453–458.

(32) Shchavlev, A. E.; Pankratov, A. N.; Borodulin, V. B.; Chaplygina, O. A. DFT study of the monomers and dimers of 2-pyrrolidone: equilibrium structures, vibrational, orbital, topological, and NBO analysis of hydrogen-bonded interactions. *J. Phys. Chem. A* **2005**, *109*, 10982–10996.

(33) Bánhegyi, G.; Ángyán, J.; Kajtár, M. Structure and ring inversion of 2-pyrrolidone. Semiempirical quantum chemical study and analysis of X-ray data. *Collect. Czechoslov. Chem. Commun.* **1986**, *51*, 249–263.

(34) Katrusiak, A. Structure of 1, 3-cyclopentanedione. *Acta Crystallogr. C* **1990**, *46*, 1289–1293.

(35) McMahon, T. J.; Bailey, J. R.; Bird, R. G. Structure and dynamics of succinic, methylsuccinic and itaconic anhydrides in the gas phase. *J. Mol. Spectrosc.* **2018**, *347*, 35–40.

(36) Jahn, M. K.; Obenchain, D. A.; Nair, K. R.; Grabow, J.-U.; Vogt, N.; Demaison, J.; Godfrey, P. D.; McNaughton, D. The puzzling hyper-fine structure and an accurate equilibrium geometry of succinic anhydride. *Phys. Chem. Chem. Phys.* **2020**, *22*, 5170–5177.

(37) Vogt, N.; Khaikin, L. S.; Grikina, O. E.; Karasev, N. M.; Vogt, J.; Vilkov, L. V. Flexibility of the saturated five-membered ring in 2, 5-pyrrolidinedione (succinimide): electron diffraction and quantum-chemical studies with use of vibrational spectroscopy data. *J. Phys. Chem. A* **2009**, *113*, 931–937.

(38) York, L.; Sorrells, C.; Dim, C. A.; Crabtree, K. N.; Hernandez-Castillo, A. O. A Tale of Two Tails: Rotational Spectroscopy of N-Ethyl Maleimide and N-Ethyl Succinimide. *J. Phys. Chem. A* **2024**,

(39) Crabtree, K. N.; Westerfield, J. H.; Dim, C. A.; Meyer, K. S.; Johansen, S. L.; Buchanan, Z. S.; Stucky, P. A. Rotational spectroscopy of methyl tert-butyl ether with

a new Ka band chirped-pulse Fourier transform microwave spectrometer. *Phys. Chem. Chem. Phys.* **2024**, *26*, 13694–13709.

(40) Pickett, H. M. The fitting and prediction of vibration-rotation spectra with spin interactions. *J. Mol. Spectrosc.* **1991**, *148*, 371–377.

(41) Dunning Jr, T. H. Gaussian basis sets for use in correlated molecular calculations. I. The atoms boron through neon and hydrogen. *J. Chem. Phys.* **1989**, *90*, 1007–1023.

(42) Peterson, K. A.; Dunning Jr, T. H. Accurate correlation consistent basis sets for molecular core–valence correlation effects: The second row atoms Al–Ar, and the first row atoms B–Ne revisited. *J. Chem. Phys.* **2002**, *117*, 10548–10560.

(43) Becke, A. Density-functional thermochemistry. III. The role of exact exchange. *J. Chem. Phys.* **1993**, *98*, 5648.

(44) Frisch, M. J.; Pople, J. A.; Binkley, J. S. Self-consistent molecular orbital methods 25. Supplementary functions for Gaussian basis sets. *J. Chem. Phys.* **1984**, *80*, 3265–3269.

(45) Chai, J.-D.; Head-Gordon, M. Long-range corrected hybrid density functionals with damped atom–atom dispersion corrections. *Phys. Chem. Chem. Phys.* **2008**, *10*, 6615–6620.

(46) Weigend, F.; Ahlrichs, R. Balanced basis sets of split valence, triple zeta valence and quadruple zeta valence quality for H to Rn: Design and assessment of accuracy. *Phys. Chem. Chem. Phys.* **2005**, *7*, 3297–3305.

(47) Matthews, D. A.; Cheng, L.; Harding, M. E.; Lipparini, F.; Stopkowicz, S.; Jagau, T.-C.; Szalay, P. G.; Gauss, J.; Stanton, J. F. Coupled-cluster techniques for computational chemistry: The CFOUR program package. *J. Chem. Phys.* **2020**, *152*, 214108, _eprint: https://pubs.aip.org/aip/jcp/article-pdf/doi/10.1063/5.0004837/16669743/214108_1_online.pdf.

(48) Frisch, M. J. et al. Gaussian 16 Revision C.01. 2016; Gaussian Inc. Wallingford CT.

(49) Jorge, F. E.; Canal Neto, A.; Camiletti, G. G.; Machado, S. F. Contracted Gaussian basis sets for Douglas–Kroll–Hess calculations: Estimating scalar relativistic effects of some atomic and molecular properties. *J. Chem. Phys.* **2009**, *130*.

(50) Watson, J. K. G. Determination of centrifugal distortion coefficients of asymmetric-top molecules. *J. Chem. Phys.* **1967**, *46*, 1935–1949.

(51) Vishnevskiy, Y. V.; Vogt, N.; Korepanov, V. I.; Ivanov, A. A.; Vilkov, L. V.; Kuznetsov, V. V.; Mahova, N. N. Molecular structure of N-chlorosuccinimide studied by gas-phase electron diffraction and quantum-chemical methods. *Struct. Chem.* **2009**, *20*, 435–442.

(52) Pyykkö, P. Spectroscopic nuclear quadrupole moments. *Molecular Physics* **2001**, *99*, 1617–1629.

(53) Legon, A. C.; Thorn, J. C. Equilibrium nuclear quadrupole coupling constants from the rotational spectrum of BrCl: a source of the electric quadrupole moment ratios Q (^{79}Br)/ Q (^{81}Br) and Q (^{35}Cl)/ Q (^{37}Cl). *Chem. Phys. Lett.* **1993**, *215*, 554–560.

(54) Pejlovas, A. M.; Oncer, O.; Kang, L.; Kukolich, S. G. Microwave spectrum and gas phase structure of maleimide. *J. Mol. Spectrosc.* **2016**, *319*, 26–29.

(55) Villamañan, R. M.; Lopez, J. C.; Alonso, J. L. Rotational spectrum and ring-puckering vibration in 2, 5-dihydrofuran. *Chem. Phys.* **1987**, *115*, 103–108.

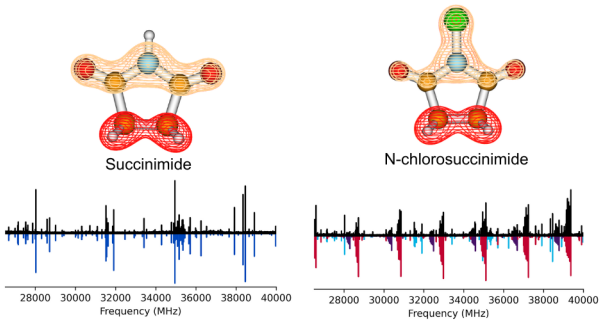
Succinimide
N-chlorosuccinimide
28000 30000 32000 34000 36000 38000 40000
Frequency (MHz)
28000 30000 32000 34000 36000 38000 40000
Frequency (MHz)